

# Chapter 6

## Photovoltaic Source Emulation

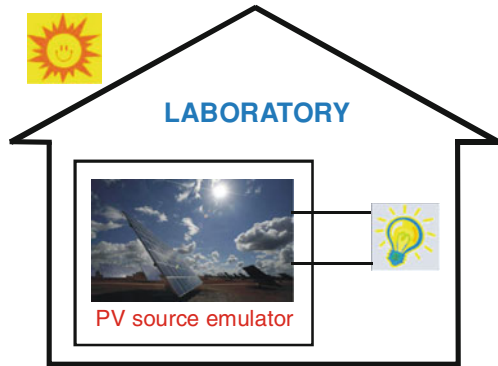
### 6.1 Introduction

Up to now, it has been amply demonstrated the possibility for solar cells, modules, or fields to be modeled theoretically. However, the obtained results require a validation through suitable experiments involving the PV source as well as various kinds of loads, such as resistive loads, DC motors, storage batteries, and inverter-connected loads with their maximum power point trackers (MPPT).

The experimental analysis of PV systems, especially when power electronic conversion circuits are present, is a very difficult challenge. Indeed, a real plant needs a wide outer surface and high costs; moreover, its produced energy is strongly dependent on uncontrollable weather conditions. Finally, the necessary investment to set up an experimental plant can be made more severe by the continuous evolution of the involved technologies. Therefore, alternative solutions to the use of an actual outdoor plant for managing problems like tests on MPPT, appropriate control for interfacing the PV generator to the grid or load, and so on, have to be taken into consideration.

For PV sources with power up to hundreds of watts, this difficulty can be overcome creating artificial environmental conditions inside the laboratory. This solution may imply the use of the so-called *solar simulators*, i.e., suitable lamps that have a spectrum reproducing the natural sunlight and can replace the Sun for repeatable and accurate indoor testing of the I–V characteristics of PV generators. The characteristics of the spectrum to be reproduced are described in [Sect. 1.2](#). The problem related to the use of such systems is tied to the relevant power requirement and heat generation. As an example, up to about a decade ago, to get an irradiance of  $1000 \text{ W/m}^2$  on a 50 W PV panel, an electric power of about 10 kW is needed; while for a 2 kW PV array, the required electric power is even about 400 kW. The use of novel discharge lamps allows to obtain a better efficiency, but the produced spectrum differs from that produced by the sun light. Recently the use of light emitting diode (LED) solar simulators has been proposed to mimic the spectrum and intensity of natural sunlight; this is a quite cheap and efficient

**Fig. 6.1** Conceptual scheme illustrating the scope of a PV source emulator



solution in a market dominated by very expensive and high power devices. Generally, the *solar simulators* present some problems with achieving a uniform distribution of the irradiance.

For all these reasons, when higher powers are involved, the most appropriate solution is the use of other kind of devices, that will be referred, hereafter, as PV source emulators, or simply PV emulators.

An emulator is, in general, intended as a system that duplicates the functions of an equipment using a different hardware. Such a system differs from computer simulation tools that concern abstract models of the equipment to be simulated.

The possibility to setup an emulator of a PV generator, in which voltage and current behave as in the real source, is very advantageous.

The PV source emulator should show the same electrical characteristics (power, voltage, current) of a photovoltaic source, including their dependence on weather conditions, partial shadow, and dynamics, allowing the user to manage a virtual plant. Such an experimental facility would allow measurements and tests to be carried out, without the constraints of the real environmental conditions and, above all, more cheaply, since the use of an actual PV array is avoided. So, for example, the optimal choice and design of the power converter interfacing the PV generator to the utility or load and the study of all the problems related to the power electronic control would be performed more rapidly and effectively. This is a very important issue, especially in consideration of the more and more growing interest in the application of renewable energy sources in distributed generation.

Figure 6.1 synthesizes, in a perceptual way, the basic idea and scope of a PV source emulator.

Summarizing the contents of this chapter, the basic concepts of the PV source emulators are given with specific details of the possible hardware topologies and control issues. Aspects related to rated power, modularity, and dynamics are discussed, and finally some examples of commercial solutions are described as well.

## 6.2 PV Emulators: Concepts and Realization

The emulation of a PV generator is tied to two main tasks: the first one is the knowledge of the I–V characteristics of the generator, the latter consists in their reproduction by suitable power amplifiers, which defines the maximum power that can be generated.

In general, the I–V characteristics of a PV array can be deduced by a PV cell model, otherwise a data base can be set up by measuring I–V curves in different environmental conditions. With regard to this first task, an extensive discussion on PV source modeling and parameters identification has been given in the previous chapters.

As for the second task, a broad variety of realizations for PV emulators have been proposed in the technical literature, already as from the beginning of the 1980s.

Among the basic ideas suggested in the past for the setup a PV source emulator there are:

1. the modification of a voltage source so that its internal resistance is variable according to an exponential law with current;
2. the amplification of the current and voltage of a single cell;
3. the definition of a PV generator equivalent circuit formed of an equivalent constant current source and a diode resistor network.

All these methods have shown a limited flexibility in readily follow the influence of solar irradiance, temperature, and other parameters of the PV generator. Moreover, some of these methods are unpractical for the emulation of PV sources in the range of kW. For example, the method at point three would require the use of unacceptable number of diodes and high power current sources.

For all these reasons, the research in the field of PV emulators has been onwards oriented to the use of active power sources suitably driven to give characteristics close to reality.

Conceptually, modern PV source emulators are power electronic converters whose output voltage and current are controlled so as to reproduce the electrical behavior of PV generators.

In the following sub-sections, the key issues of PV emulators proposed in the technical literature are described both considering the chosen hardware solutions and the control issues.

### 6.2.1 Power Stage: A Survey of Proposed Solutions

A first rough classification of PV emulators, on the basis of their hardware structure, can be made considering the power amplifier used to realize its operation.

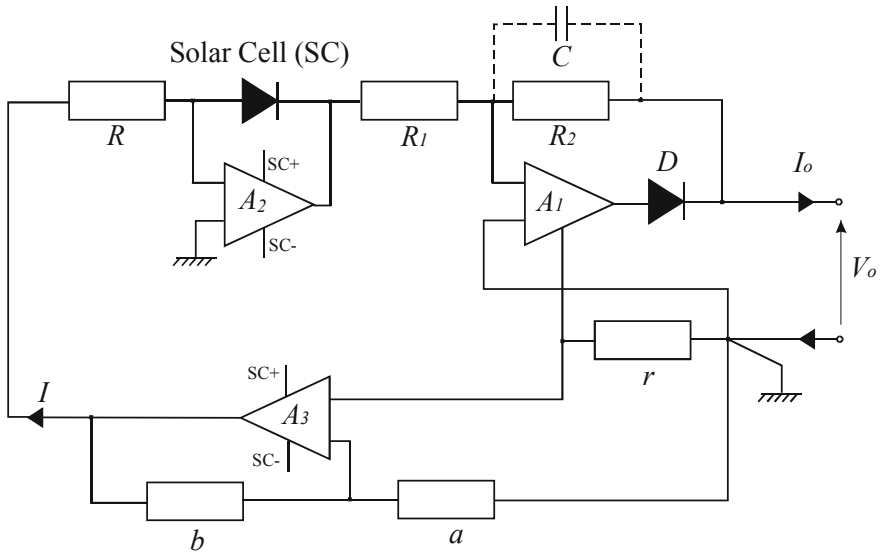


Fig. 6.2 Scheme of the PV source emulator proposed by Baert

In the technical literature realizations with operational amplifiers, series regulators, and switching converters have been proposed. Some typical examples are discussed in Sects. 6.2.1.1, 6.2.1.2, and 6.2.1.3, respectively.

### 6.2.1.1 Circuits Based on Operational Amplifiers

One of the earliest contributions on PV source emulators is due to Baert (1979) that proposed a circuit having the effect of virtually increasing the area of a small reference solar cell. This circuit has been intended for studies on both inverters and battery storage systems.

The circuit is based on power operational amplifiers, as shown in Fig. 6.2. In particular, the amplifier  $A_1$  allows the output solar cell voltage to be multiplied by a factor  $-R_1/R_2$  that is equivalent to consider a string of  $R_1/R_2$  cells in series.

The output current is sensed by a low value resistance  $r$  by which it is transformed into a voltage, then it is fed back into the cell by the amplifier  $A_3$ ; therefore, the new output current is the reference cell current multiplied by a factor  $aR/br$ . This situation is equivalent to consider  $aR/br$  strings in parallel. With a suitable choice of the components' values an area multiplication factor up to  $10^4$  can be obtained.

The capacitor  $C$  is used as a bandwidth limiter to suppress high frequency oscillations, while the diode  $D$  is used to protect the output from undesired reverse current or voltage.

A similar approach is followed by Nagayoshi (2004) that proposes a multi I-V magnifier circuit whose elementary unit is based on a DC linear amplifier.

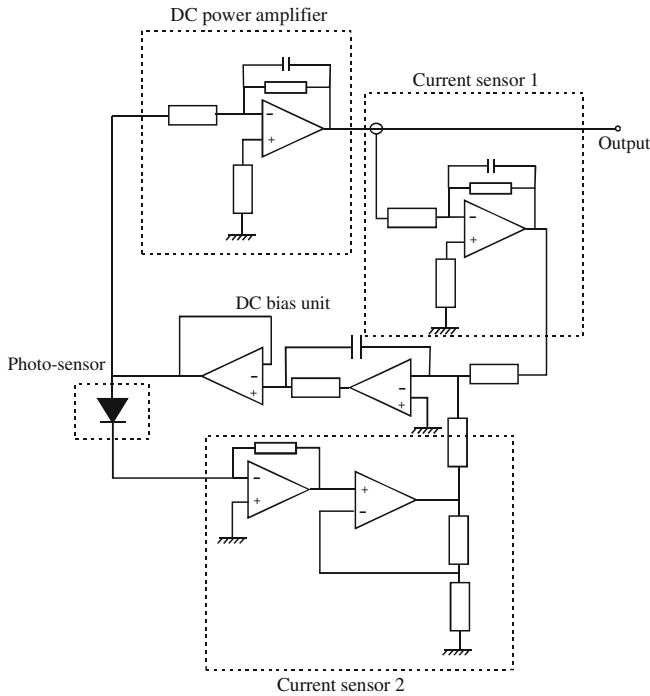


Fig. 6.3 Scheme of the PV source emulator proposed by Nagayoshi

The circuit uses a small PV cell as an I–V generator and provides a separate amplification of voltage and current to realize the operation as a PV emulator. The scheme of the I–V magnifier is illustrated in Fig. 6.3.

It is possible to observe that a DC power amplifier increases the output voltage of the small PV cell (obtained by a pn photo-sensor illuminated by a LED light), while the operational point is controlled by the feedback signal coming from a current sensor placed at the simulator output. In detail, the output current of the PV emulator  $I_{out}$  and the pn photo-sensor current  $I_{ph}$  is monitored by the current sensors 1 and 2, respectively. The output voltage of the current sensor 2 is kept equal to the voltage output of the current sensor 1 at any time by the feedback control. Therefore the current gain is given by:

$$A_I = I_{out}/I_{ph} = G_2/G_1 \tag{6.1}$$

where

$$G_1 = V_{s1}/I_{out} \tag{6.2}$$

$$G_2 = V_{s2}/I_{ph} \tag{6.3}$$

Being  $G_1$  and  $G_2$  the gains of the current sensors 1 and 2, respectively and  $V_{s1}$  and  $V_{s2}$  the output voltages from the current sensors 1 and 2, respectively. According to these equations, it is possible to observe that the current gain is independent of the voltage gain, defined by the power amplifier.

In this system, the temperature dependence of solar source is implemented by a temperature control of the photo sensor.

Several I–V curves were obtained by the described PV emulator using a power variable resistor as a load. These curves are proportionally magnified to  $x$ -axis by changing the voltage gain of the DC power amplifier and to  $y$ -axis by changing the current gain.

The output on series connection of emulation basic units has suggested the possibility for the system to emulate shading effects on a PV source.

The two above described realizations are both based on a physical sample of the source to be emulated. The use of the operational amplifier allows voltage and current delivered by the source to be amplified, their maximum values are limited only by the amplifier performance. Moreover, the operational amplifier has a good bandwidth to reproduce correctly transients. On the other hand, parasitic phenomena, tied to junction capacitance or wires inductance, can be reproduced correctly only with reference to the PV cell used as sample. As a matter of fact, the series (parallel) connection of PV cells lessens (increases) the junction capacitance value and increases (lessens) the parasitic inductance; hence, a mere multiplication of the voltage or of the current cannot take into account these effects. Finally, partial shading phenomena can be emulated only by using more emulators.

In order to overcome the limited flexibility of common PV emulation methods in readily simulating the influence of weather and PV source parameters, Easwarakhanthan et al. (1986) proposed a microcomputer controller emulator based on a programmable DC voltage source, a programmable multimeter and a power amplifier. In this system the operating points are approached for changes in load, solar irradiance, temperature, and in various PV module/array parameters according to a linear interpolation iterative technique.

In detail, a computer calculates the output current and voltage at the intersection between the I–V curve of the PV source and a straight line between two points subsequently processed on the load operating curve. Then it programs the DC voltage generator to apply the calculated voltage to the load, acquires the measured current by the multimeter, and compares current with that calculated.

A waiting loop is enabled when the relative difference between measured and computed currents reaches a desired limit.

A principle scheme of this emulator is shown in Fig. 6.4.

It should be observed that, the operation of the described system requires an a priori knowledge of the connected load operating curve.

**Fig. 6.4** Principle scheme of the PV source emulator proposed by Easwarakhanthan et al

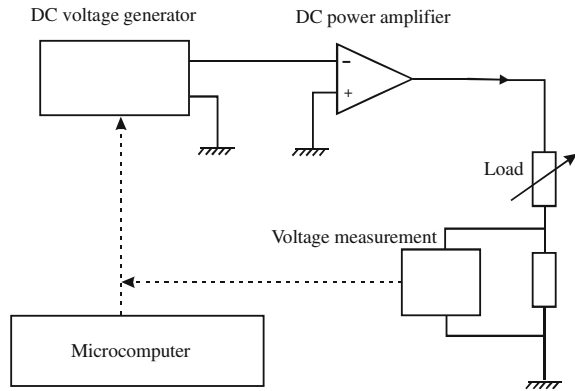
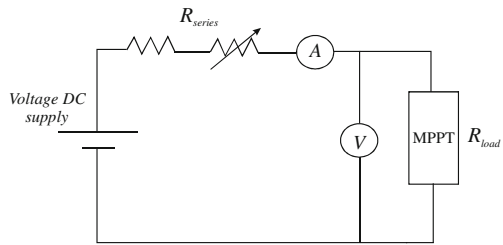


**Fig. 6.5** Principle scheme of the PV source emulator proposed by Mukerjee and Dasgupta



**6.2.1.2 Circuits Based on Linear Regulators**

In this kind of circuits, the output voltage is obtained by a DC supply and a series component that causes a voltage drop. As a consequence, the output voltage is always lower than the voltage of the DC supply. This effect can be obtained by a power BJT that is polarized in active region and works as a class A amplifier. However, a similar effect, although quite rough, can be also obtained with a series resistor.

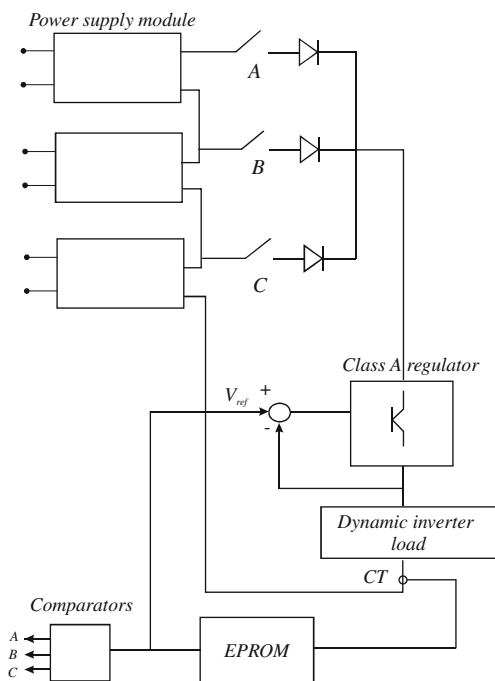
A low cost circuit used as a PV emulator for testing MPPT has been proposed by Mukerjee and Dasgupta (2007). It is based on a variable voltage DC power supply with a variable resistor at its output. This circuit gives a behavior with a peak on the power curve, similar to that of a PV generator, allowing the tracker to lock on to.

A principle scheme of the system is given in Fig. 6.5.

With reference to Fig. 6.5, if the resistance indicated as  $R_{series}$  is fixed, when  $R_{load}$  varies from its minimum to its maximum value, the voltage across it plotted against current gives a linear trend with a negative slope.

The power dissipated on  $R_{load}$  reaches its maximum when the voltage drop on such a resistance is about half the applied DC voltage, corresponding to the  $V_{oc}$  of the emulated PV generator. Therefore, the P–V curve gets a maximum similar to the P–V curve generated by a PV source. The MPPT will track this maximum.

**Fig. 6.6** Scheme of the PV source emulator proposed by Lloyd et al



In order to take into account variations in temperature, the value of the input DC supply voltage is modified, considering that, when temperature changes, the open circuit voltage changes significantly.

For increasing or decreasing the short-circuit current, the value of  $R_{\text{series}}$  is suitably modified, assuring that a finite resistance is always in series with the power supply, to avoid its possible damage.

An interesting solution using the combination of a class A regulator and several DC supplies that can be connected to the regulator by switches has been proposed by Lloyd et al. (2000). In particular, a modular design has been followed to setup a PV source emulator, whose single power unit is capable of delivering a maximum power of 400 W.

In order to take into account the real PV source's behavior, a set of precalculated I-V curves for specified values of solar irradiance and temperatures has been used. These curves are loaded into a EPROM used as a look-up-table (LUT).

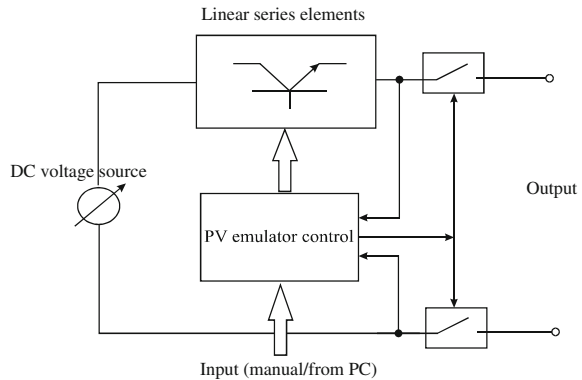
The I-V curves have been calculated on the basis of a double diode model with reference to both a polycrystalline and amorphous silicon (a-Si) PV panels.

The hardware implementation of this system is depicted in Fig. 6.6.

The class A regulator produces an output voltage, according to the I-V characteristics contained within the EPROM, to test the inverter supplied by the PV source.



**Fig. 6.7** Schematic description of the PV source emulator proposed by Haeberlin and Borgna



The regulator is provided with a current control allowing additional power units to be connected in parallel, to obtain higher output current and a close tolerance current sharing.

The static switches, indicated as A, B, and C in Fig. 6.7, are automatically selected to make the regulator operate within its range, as the working point sweeps through the I–V curve. Power supply modules can be connected in series or parallel to meet the I–V specifications of the PV inverter under test.

This emulation system permits two operation modes, as:

- I. Current regulator: in this case the voltage is measured and input to the EPROM that gives a desired value of the load current.
- II. Voltage regulator: in this case the EPROM gives the reference voltage,  $V_{ref}$ .

In the first case the measured voltage is used to switch the power supplies while, in the second case, the reference (or desired) voltage is used.

An interesting high power linear PV source emulator (for powers up to tens of kW) is proposed by Haeberlin and Borgna (2004) to be used for measurement on PV inverters, including MPPT efficiency.

It is based on a controlled linear current source characterized by high stability and no interaction with the power electronic circuits under test.

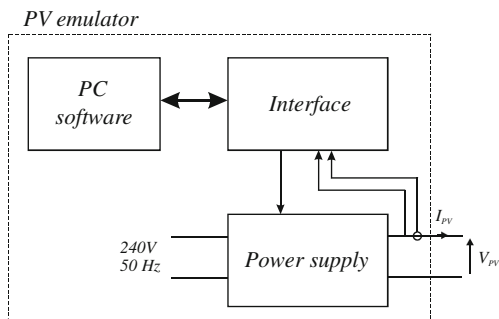
The principle scheme of such a device is depicted in Fig. 6.7.

It is possible to observe the presence of two series isolation switches used to provide galvanic isolation at the output of the PV emulator when it is not working.

The choice of a linear design, in this case, is considered appropriate for two main reasons: the better dynamic response and the absence of internally generated high frequency voltages, since no PWM switching occurs, that is an advantage as far as the electromagnetic compatibility is concerned.

On the other hand, the linear design implies a serious drawback; in particular, if the emulator is operated close to the short-circuit condition with high values of the voltage source a big amount of power will be dissipated in the linear series elements.

**Fig. 6.8** Block diagram of the PV source emulator proposed by Khouzam and Hoffman



Anyway, this condition is uncommon and the power losses can be reduced by an appropriate choice of the feeding source voltage level and by an appropriate reduction of the current close to the short circuit point. These power losses, however, remain higher than the power lost in switching converters described in the next section.

In this emulator the power variation is imposed by varying the operating current. This operating mode reproduces solar irradiance variation with constant temperature.

### 6.2.1.3 Circuits Based on Switching Converters

The PV source emulators, whose hardware structure is based on power electronic converters, are the majority in the technical literature. The reason for their success relies in the following considerations.

A DC linear amplifier needs, in general, a large heatsink and its conversion power losses approach the 100 % when the PV emulator supplies the short-circuit current. In a DC/DC converter the power devices are operated considering only two fundamental states: the *on* state in which the voltage of the power switch is null and the *off* state in which, in turn, the current is null. In both cases, in principle, there is no dissipated power; only during transitions between *on* and *off* states and vice versa a low amount of power, dependent on the switching frequency is dissipated. As a consequence, the overall efficiency is expected to be very high and a smaller size emulation unit can be set up.

A PV emulator realization based on a switched mode step-down converter, operating under computer control, is due to Khouzam and Hoffman (1996). This system can emulate a PV generator in real time, accounting for the characteristics of any array, its size, as well as specific irradiance and temperature conditions, and PV aging.

All these data can be entered into the computer, so that the converter output is controlled to reproduce the corresponding operating point.

In detail, the system is composed of a preregulator, a switch-mode step-down DC/DC power converter producing up to 100 W (power supply), a computer interface and a modeling and control software.

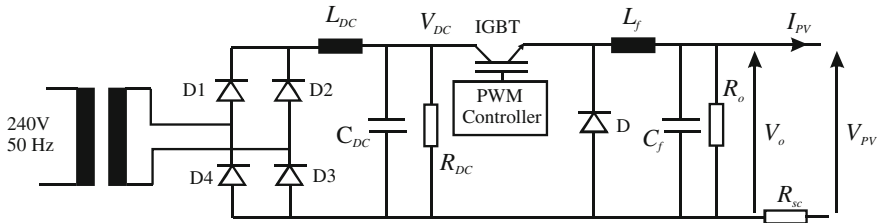


**Fig. 6.9** Details of the power supply block (PV emulator proposed by Khouzam and Hoffman)

The novelty of the approach in the setup of this emulator was the use of a mathematical modeling to describe the output characteristic of the PV source.

Figure 6.8 shows the block diagram of the PV emulator.

The details of the block indicated as power supply in Fig. 6.8 are illustrated in Fig. 6.9. In particular, the mains voltage is stepped down by an isolation transformer, rectified, and smoothed to create an unregulated DC voltage,  $V_{DC}$ ; this voltage is the input for the DC/DC step-down switching converter, operated at 50 kHz, that gives a regulated DC voltage ranging from 0 to 100 V.

The shunt resistor  $R_o$  is used to allow a continuous conduction mode operation of the DC/DC converter (i.e., an operation where the current in the converter inductor never goes to zero between switching cycles) even for  $I_{PV}$  equal to zero.

The series resistor  $R_{sc}$  is used to provide a degree of current limiting if the output is in short circuit.

By implementing the PV model equations in the control software, the output voltage of the DC/DC step-down converter is driven to follow the law  $V_{PV} = f(I_{PV})$ . In detail, the output current of the converter is firstly measured, then the corresponding theoretical voltage is calculated.

The process is repeated iteratively and within a few milliseconds until the correct output voltage and current are within a small tolerance for a given load and a specified set of PV parameters. As for these parameters, as well as solar irradiance, temperature, and aging conditions, they can all be selected and modified before and during operation. Furthermore, the PV array I–V curves may be defined in terms of either theoretical array parameters or interpolation between measured values of a real array.

Another interesting topology of PV source emulator has been proposed by Sanchis et al. (2003). Its main idea is to both measure the real and dynamic evolution of the characteristic curves of a PV generator at outdoor operation and then to reproduce them at the laboratory for inverters and MPPT testing.

A global description of the system is given in Fig. 6.10, where it is possible to observe that the whole system consists of an electronic converter, a microcontroller and a data storage unit. A measuring card is also included in the power converter with the aim to both measure, by suitable sensors, the I–V curves of a PV array and to implement the control loops.

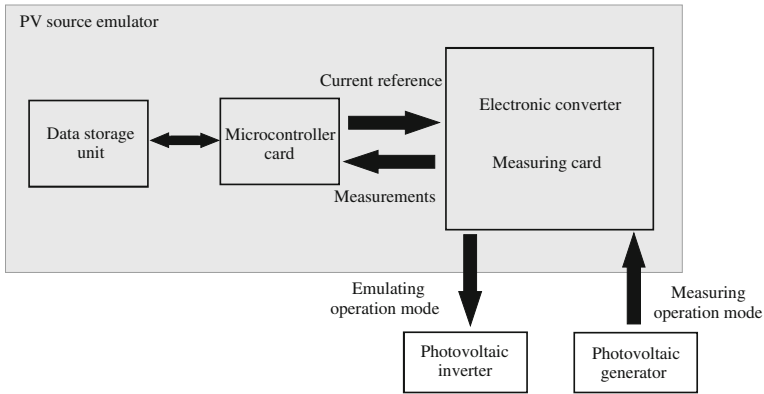


**Fig. 6.10** Global description of the PV source emulator proposed by Sanchis et al

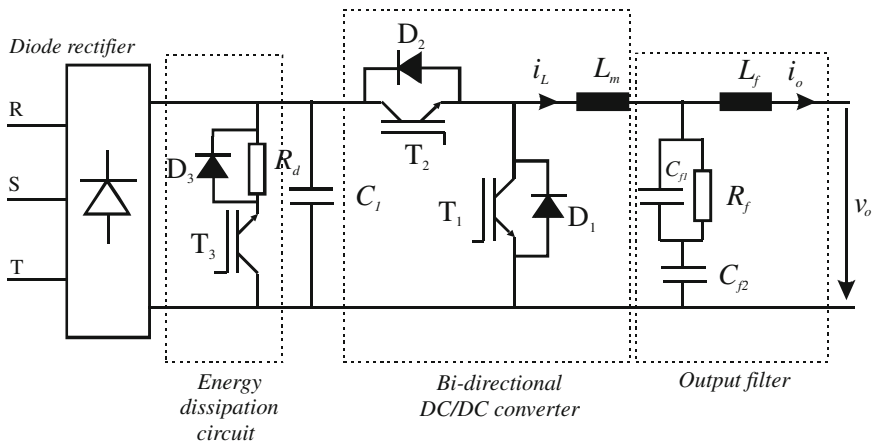


**Fig. 6.11** Circuit scheme of the power stage of the PV source emulator proposed by Sanchis et al

The circuit scheme of the emulator's power stage is given in Fig. 6.11.

It can be noted that the emulator is realized by a bi-directional IGBT-based DC/DC converter that allows two different operation modes, i.e., measurement and emulation, with the evident advantage to combine both the planned working modes in a single equipment.

When the system runs in emulating mode, the power converters behave as a power source; in particular, it is operated as a buck converter supplied by the power grid via the diode rectifier.

On the contrary, when the system runs in measuring mode, the converter behaves as a variable loads and it is operated as a boost converter, supplied by a PV generator.

The system prototype can measure and emulate the behavior of a PV generator up to 15 kW and has the capability to measure continuously three time per second

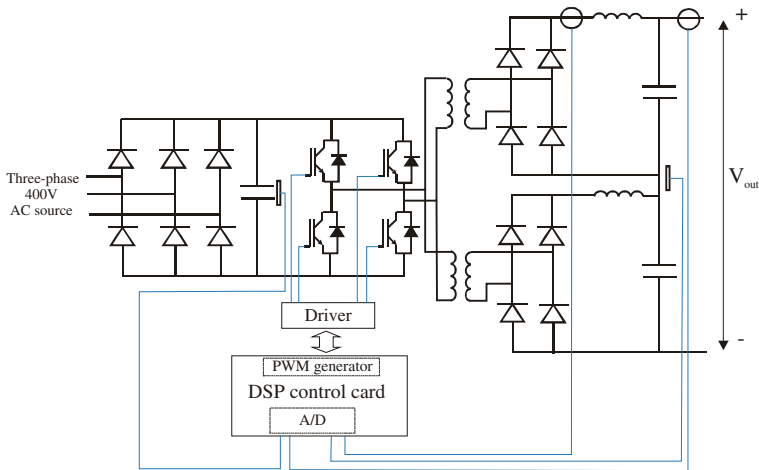


**Fig. 6.12** Circuit scheme of the PVAE proposed by Martín-Segura et al

the full I–V curves up to seven PV arrays, that means to store approximately 10800 curves per hour in the database.

The usefulness of this equipment is the possibility to carry out a systematic characterization and testing of PV inverters and MPPT under any varying and nonideal operating condition.

A PV emulator based on a topology different from a single stage DC/DC converter is proposed by Martín-Segura et al. (2007). In particular, this photovoltaic array emulator (PVAE) is a multi-stage DC/DC converter composed of a DC/AC full bridge inverter, a high frequency transformer, and an uncontrolled rectifier for each secondary transformer winding. With this choice, a more secure operation, due to galvanic isolation, and high voltages are allowed.

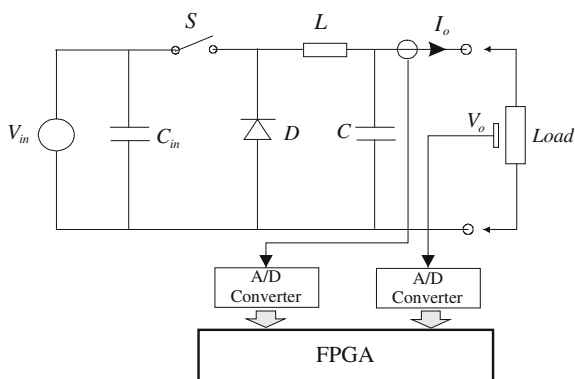
The high output voltage availability allows PV arrays configurations, like those used in centralized technology inverter (see Sect. 3.5, Fig. 3.19), to be emulated.

The electrical scheme of the emulator is shown in Fig. 6.12. The full bridge converter is fed by a rectified three phase 400 V supply. In order to increase the output voltage two transformers, with the primary connected in parallel and the secondary in series, are used. The inverter is based on IGBTs commutated at 18 kHz. The converter output is obtained on the basis of a defined, simplified I–V curve suitably implemented on a DSP control card. The emulator prototype has a rated power of 4 kW and allows testing PV inverters with an input 0–650 V and 0–7 A.

Recently, PV emulators based on DC/DC converters controlled by Field Programmable Gate Arrays (FPGAs) have been proposed. The system developed by Koutroulis et al. (2009) is worth to be considered.

The hardware structure is based on a simple buck converter whose control is obtained by an FPGA-based unit, operating according to the PWM principle. In Fig. 6.13 the scheme of this PV simulator is shown.

**Fig. 6.13** Circuit scheme of the PVAE proposed by Koutroulis et al



It is possible to observe that it is composed of the DC/DC switching converter and the control system comprising the FPGA unit, the analog to digital (A/D) converters, and the voltage and current sensors.

The advantage of an FPGA in terms of flexibility, due to its reprogramming capability and reconfigurable logic, allows the emulator to be adapted to any change. Therefore, the emulation of several types of PV generators is permitted.

In general, FPGA boards are characterized by fast computational features and make the implementation of parallel architecture feasible, thus obtaining a reduction of the control algorithm execution time.

If compared with processor-based implementations of PV emulators, the FPGA-based system contributes to a rapid prototyping since the VHDL code, used to configure the FPGA board, can be entered in a simulation routine to assess the control algorithm performance, before the hardware prototype construction.

Moreover, the high frequency operational features of the FPGA devices allow a PWM control unit architecture giving an increased power converter switching frequency to be implemented. Therefore, a reduction of the converter size (and cost) is achievable since it is primarily tied to the inductor magnetic material size which is, in turn, inversely proportional to the converter switching frequency.

The considered emulator reproduces the I–V curve of a given PV generator operating under any condition of irradiance and temperature. It has the flexibility to be operated either with real-time measured values of  $T$  and  $G$ , coming from temperature and solar irradiance sensors or with user-defined values of  $T$  and  $G$ , entered to the PV emulator in a digital format through a PC port. The developed prototype uses a power MOSFET rated 60 V and 50 A and a PWM switching frequency of about 50 kHz.

From this brief survey of PV emulators' topologies, it is possible to conclude that the most used solution is based on the use of DC/DC switching converters. As a matter of fact, this solution permits a simple realization, a good efficiency, and an accurate reproduction of the I–V curves both in steady state and dynamic conditions.

### 6.2.2 Control Stage: PV Behavior Implementation

The control law of a PV emulator is oriented to establish, for any environmental and load condition, an operating point lying on an I–V characteristic of the real photovoltaic array to be emulated.

As previously stated, theoretical models of a PV source based on equivalent circuits can be used to describe a complete set of I–V characteristics. A further option consists on the use of a database set up by measuring I–V curves in different environmental conditions, as a reference.

Another way to regulate the emulator output, implemented by some authors that have developed PV emulators based on operational amplifiers, is obtained by forcing the operating point of the sample cell by auxiliary circuits. This approach makes without the direct evaluation of either the I–V mathematical relationship or the characteristics' measurement

According to this method, the electrical behavior of the PV generator is considered by imposing a change in the operating point through a suitable and independent amplification of current and voltage at the output of a small PV cell, as explained in Sect. 6.2.1.1.

In the more common and promising PV emulators realized by switching converters, the output regulation is mostly based on I–V curves. With reference to these PV emulators, some general issues related to the control implementation are given in the next subsection.

#### 6.2.2.1 I–V Curve-Based Regulation: Implementation Issues

The output of a PV emulator based on a switching converter is adjusted in real time by the control system so to reproduce the external I–V characteristics of a PV generator. As a result, from the PV inverter and load point of view, the PV emulator behaves as the PV source, as long as its characteristics are suitably programmed (usually off-line) in the controller.

The general principle of the converter control can be schematized as shown in Fig. 6.14. In particular, for the most common case of a DC/DC converter, the duty cycle regulation is performed on the basis of the output current detection and the definition of reference voltage from the established I–V behavior of the PV source.

In the case shown in Fig. 6.14, the interface board has the task of transforming, isolating and filtering the current and voltage signals coming from the current, and voltage transducers, respectively.

Both current and voltage at the output of the converter are sent to the PWM generator as feedback signals, while the output current is entered in the control board. Here, the current is used to calculate the corresponding reference voltage which is sent to the PWM generator after A/D conversion and filtering.

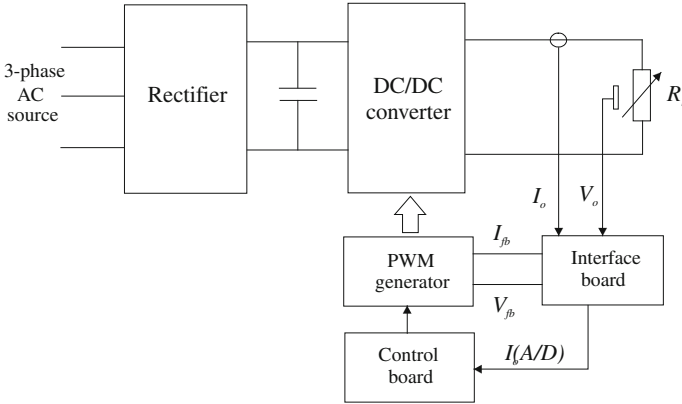


**Fig. 6.14** General scheme of the converter control principle

Closed loop control is the preferred solution, even if the literature exhibits examples of open loop controls based on the real-time measurement of the load resistance, as in Zeng et al. (2002).

The PV source behavior definition within the control, i.e., the I–V curve representation, follows, as previously anticipated, two main approaches:

- the model-based approach;
- the measurement-based approach.

In the model-based representation of the PV characteristics, it is assumed that all the PV source theoretical parameters are available; therefore, the output voltage is calculated using these parameters and, in addition, solar irradiance and temperature.

In order to exploit the simplicity and flexibility of a linear model, some authors, simplify the PV source model used for the representation of the I–V curve. In particular, they consider the I–V characteristics as formed by the two lines obtained joining the remarkable points ( $V_{oc}$ ,  $V_{MPP}$ ,  $I_{MPP}$  and  $I_{sc}$ ), according to Eqs. (6.4 and 6.5).

$$I = \frac{V_{MPP} - V_{oc}}{I_{MPP}} \cdot V + V_{oc} \quad (6.4)$$

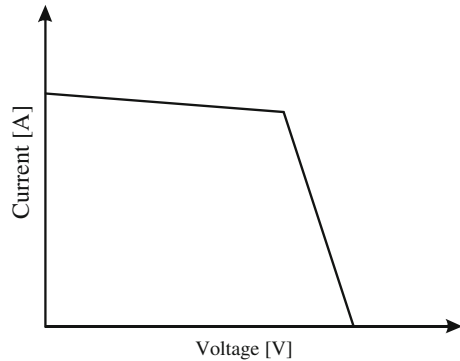
$$I = \frac{V_{MPP}}{I_{MPP} - I_{sc}} \cdot V - \frac{V_{MPP} \cdot I_{sc}}{I_{MPP} - I_{sc}} \quad (6.5)$$

The shape of the linearized I–V curve is shown in Fig. 6.15.

In general, the use of simplifying approximations, when do not introduce significant errors, is advantageous since it implies a reduced calculation complexity. This simplification is especially applied when the resulting I–V curve is stored in a LUT, which is part of a digital control system with limited resources in terms of hardware capability.



**Fig. 6.15** Shape of the linearized I–V curve



In the measurement-based approach for I–V curve representation it is possible to distinguish:

- methods using interpolation between measured values of a real PV generator;
- methods using the full PV curve measurement.

In the first case (it is assumed that the theoretical parameters of the PV source are unavailable), three measured points are needed, i.e., the open circuit point, the short circuit point, and the maximum power point, being the measurements conducted in reference conditions for temperature and solar irradiance.

The resulting equations will be determined for any temperature and irradiance value.

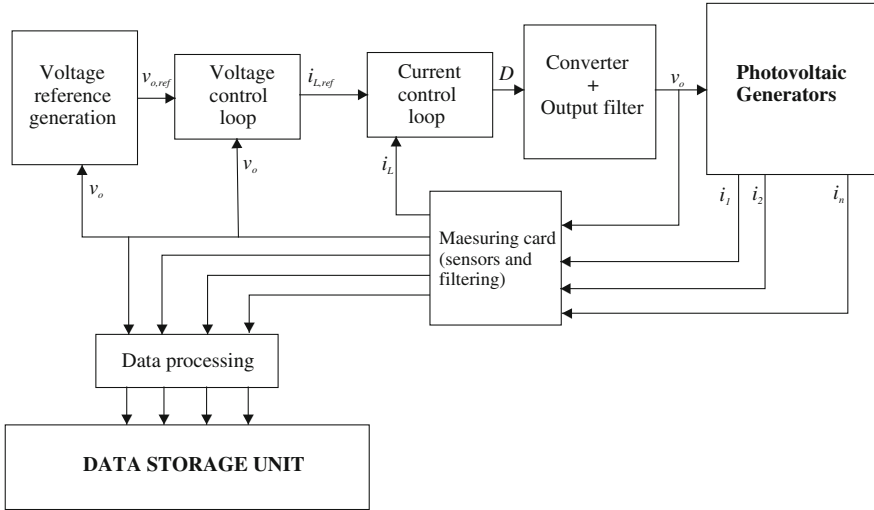
In the second case, a controlled variable load (usually the PV inverter) is needed to make the PV generator completely cover the I–V characteristics. Moreover, with this approach, a suitable storage unit is required to store the measured data that will be organized and classified by a data processing unit to be used for emulation purpose. An appropriate quickness and capability to store a large amount of data are required to the used database.

Figure 6.16 illustrates the scheme of a systems used for the real-time measurement of a PV generator full I–V curves (it represents the measuring operation mode of the system proposed by Sanchis et al., described in Sect. 6.2.1.3).

Regardless of the chosen approach for the representation of the I–V curves, they have to be converted into a data table and suitably stored in a memory.

It should be observed that, the chosen word length of the calculated parameters comes from a trade-off between the controller hardware resources and the accuracy required to the PV emulator.

For example, in the PV emulator shown in Fig. 6.7, the I–V curves related to 64 different values of solar irradiance, between 0 and  $1200 \text{ W/m}^2$ , are calculated using a double diode PV model. Then they are stored into a 16-bit EPROM using 4096 words for each I–V curve.



**Fig. 6.16** Scheme of a systems used for the real-time measurement of a PV generator full I-V curves

On the other hand, for the PV emulator shown in Fig. 6.13, the I-V curve of an ideal PV module, represented according to a single diode model, is quantized in 8-bit integer format, according to the following relationships:

$$V_{I8m} = V \frac{(2^8 - 1)}{V_{oc, stc} - k_T (T_{C, ref} - 25)} \quad (6.6)$$

$$I_{I8m} = I \frac{(2^8 - 1)}{I_{sc, stc} (G_{ref} / 1000)} \quad (6.7)$$

where  $V_{I8m}$  and  $I_{I8m}$  are the resulting integer values of the ideal PV module voltage and current, respectively,  $k_T$  is the open circuit voltage temperature coefficient expressed in  $V/^\circ C$  and  $T_{C, ref}$ ,  $G_{ref}$  are the PV module reference temperature and solar irradiance expressed in  $[^\circ C]$  and  $[W/m^2]$ , respectively. Then, the resulting pairs of  $V_{I8m}$  and  $I_{I8m}$  are stored in a LUT implemented in the FPGA board.

Using this ideal I-V characteristic stored in a LUT, the characteristic of the PV module can be determined for any value of temperature and solar irradiance, as defined by the operator.

With specific regard to the implementation of the PV emulator control on a FPGA board, an interesting post-layout comparison has been done in Koutroulis et al. (2009) by considering several target FPGA devices, in terms of required resources, maximum PWM frequency, maximum sampling frequency, and cost.

The obtained results are given in Table 6.1.

It is possible to note that, in all cases, the implementation of the PV emulator control occupies a relatively small percentage of the available resources, thus

**Table 6.1** Post layout comparison among different FPGA devices

FPGA device	Required resources (logic cells)	Maximum PWM signal frequency (kHz)	Maximum sampling frequency (kHz)	Cost (\$)
Virtex XC2V1000	888 out of 27648 (3 %)	313.5	78.37	252
Spartan-3 XCES50	476 out of 1728 (27.5 %)	111.54	27.88	288
Spartan-3 XCES400	412 out of 8064 (5 %)	132.49	33.12	30
Virtex-44VLX80FF1148-11	1000 out of 80640 (1.2 %)	246.2	61.55	72
Spartan-3 XCES1000	LUTs: 1708 out of 15360 (11 %)	286.84	71.71	20

permitting the integration of additional power converter control operations in the same IC. Furthermore, due to the logic cells' availability, the PV emulator control can be implemented using more bits, thus increasing the accuracy of the emulator itself.

As for the maximum PWM frequency, it can be observed that any of the considered FPGA device allows the value of 100 kHz to be exceeded. Moreover, it should be observed that such values of PWM frequency, in general higher respect the PWM frequencies achievable by commercially available DSP or microcontrollers, can be obtained at a relatively low cost.

### 6.3 Dynamics and the Arbitrary Load Problem

In order to achieve an effective real-time operation, a PV emulator should exhibit an appropriate dynamic behavior. In particular, it should rapidly converge to the desired operating point when a modification of either the load or the environmental conditions occurs.

In the technical literature, response times of PV emulators up to tens of microseconds have been found, corresponding to step variations of load or solar irradiance. For example, in Matsukawa et al. (2003), proposing a 10 kW PV emulator based on a controlled active power load (APL), a response time of about 25 ms has been measured for a step variation in solar irradiance from 1000 to 500 W/m<sup>2</sup>. The same emulator shows a response time of about 16 ms for current and about 25 ms for voltage, when a step variation of the applied load from 1 k $\Omega$  to 100  $\Omega$  occurs.

A good dynamic behaviour is particularly important in PV emulator systems including the I–V curve measurement in its operating modes, such as the system schematized in Fig. 6.10. Here, the need for making the PV generators cover

continuously their characteristics, especially along the voltage axis, has suggested to include an additional voltage loop in the control board, as shown in Fig. 6.16. This loop acts as an outer control loop that provides the reference for the inner current loop. Both loops form a cascade control structure that allows a robust and accurate control of the voltage at the terminals of the PV source.

Thanks to a high switching frequency of the power converter, a cascade control structure characterized by a high dynamics is possible. Therefore, the I–V curves can be swept and measured in a few milliseconds to obtain a real-time measurement of their evolution.

In general, the design of the PV emulators' control principle is not a simple issue, since the control system should be insensitive to all involved parameters and the emulator circuit should operate correctly regardless, for example, of the value of the load capacitance.

In other words, since the main reason for using a PV emulator is to test PV inverters, a good dynamic behavior is required to avoid interference between the control system of the emulator and the control system of the supplied power converter. This issue is referred in the literature as the “arbitrary load problem”.

The solution proposed by Ollila (1995), for a PV emulator system rated 1 kW and formed of a DC/DC step-down power converter, is based on the cascade connection of separate current and voltage controllers. Being the novelty of the approach, the special capability of the used controllers of tolerating high system gain variations.

In particular, it is observed that a low value of output emulator capacitance is required to obtain a fast dynamical response. Anyway, in presence of a loading inverter the cumulative capacitance at the emulator's output can significantly increase, leading to possible system gain variations up to 1000 times the original value.

In a DC/DC buck converter, a cascade control based on the use of conventional PIs, in particular, a fast PI-controller in the inner inductor current loop and a slower PI-controller in the outer capacitor voltage loop, allows to achieve a current limitation and a fast voltage response, as well.

Anyway, this control scheme presents a disadvantage. In detail, the integration time constant has to be set very slow to obtain a sufficient phase margin if the load capacitance is large.

On the other hand, the gain has to be small to guarantee a stable operation with low load capacitance, that implies the presence of long and large dynamical error.

Since the load is a priori undefined and no trimming is permitted in standard PI, these controllers are not considered as the best solution.

To overcome the above described issues, the use of adaptive, self tuning or fuzzy schemes is possible, which obviously implies computational demanding algorithms. On the other hand, for low cost applications, a cascade control using a voltage controller with a 45° phase lag independently from frequency is proposed whose transfer function is given in Eq. (6.8).

$$G_c(s) = \frac{1}{\sqrt{t_c s}} \quad (6.8)$$

This kind of controller is indicated as  $1/\sqrt{s}$  controller.

In Eq. (6.8)  $t_c$  is the controller time constant.

The gain of the controller described by the transfer function Eq. (6.8) decreases 10 dB/decade regardless of frequency. If the system gain decreases of 20 dB/decade and has a  $90^\circ$  phase lag, the gain margin is infinite and the phase margin is  $45^\circ$  at any frequency. This leads to a slight overshoot and a fast damping in a closed loop step response, irrespective of the value of the load capacitance.

The overall closed loop bandwidth is determined by the controller and the system time constants.

In order to practically realize this kind of controller, zero-pole pairs can be used to approximate the transfer function within a given frequency interval. A truncated zero-pole form with one zero-pole pair per decade to approximate the controller transfer function is given in Eq. (6.9):

$$G_c(s) = \frac{t_c s + 1}{t_c s} \prod_{i=1}^M \frac{10^{-i} + t_c s}{10^{-1+1/2} + t_c s} \quad (6.9)$$

where  $M$  is the frequency range expressed in decades.

The approximation of the controller transfer function given in Eq. (6.9) is just suitable for several purposes but a better representation can be obtained by locating the poles and zeros, so that the average phase error is minimized in a given frequency interval. With this approach, a phase optimal solution is found assuming the presence of an additional pole (a measuring filter) in the system transfer function.

The normalized controller transfer function, in this case, will be in the form:

$$G_{c(p.u.)} = \frac{1}{\sqrt{s}} \approx k \frac{(s - z_1)(s - z_2)(s - z_3)}{s(s - p_1)(s - p_2)(s - p_3)} \quad (6.10)$$

The practical realization of the transfer functions in Eqs. (6.9) and (6.10) is quite simple and can be handled using operational amplifiers, as shown in Figs. 6.17 and 6.18.

The digital equivalents can be obtained using, for example, pole-zero matching techniques.

In order to control the PV emulator, two of the above described  $1/\sqrt{s}$  controllers are used in a current–voltage cascade structure.

In the current loop the controller eliminates the need for adaptive control in discontinuous mode, while, in the voltage loop, it allows high values of load capacitance to be tolerated. Thus, the problem of the correct handling of an arbitrary loading converter is solved.

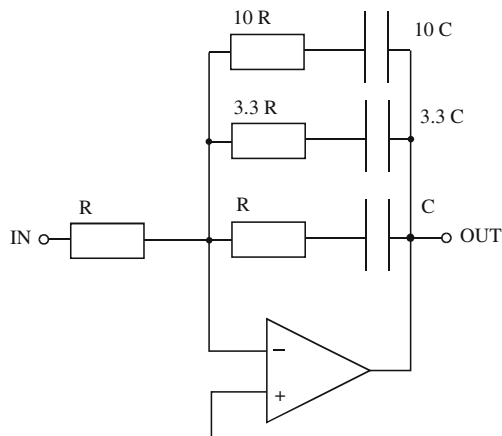


**Fig. 6.17** Practical realization of the approximate  $1/\sqrt{s}$  controller using a single operational amplifier

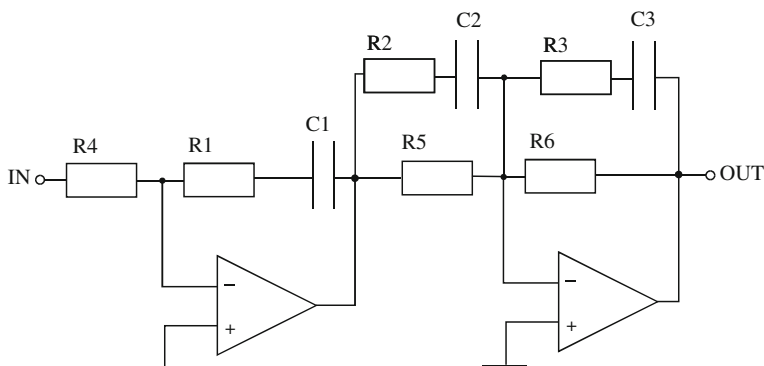


**Fig. 6.18** Practical realization of the approximate  $1/\sqrt{s}$  controller using two operational amplifiers

## 6.4 Non-Ideal Operating Conditions

The maximum flexibility and usefulness of a PV source emulator is achieved when it has the capability of reproducing correctly the PV generator electrical behavior also under nonideal operating conditions. As a matter of fact, they correspond to real and, sometimes, common situations. Therefore, testing PV inverters or MPPT techniques in such conditions gives a more realistic measure of the expected performance and can help in the improvement of current technologies and in the development of new ones.

Among the most common nonideal operating condition there is the partial shading of the PV generator.

Other possible situations are related to environmental conditions, such as rapidly changing atmospheric conditions, dawn, nightfall, etc., or to the status of the PV array such as aging, degradation due to high energy particle radiation damage (in space applications), and so on.

The natural way for taking into account these conditions is their suitable implementation in the PV emulator control stage dedicated to the representation of the I–V characteristics. This can be obtained by including the considered nonidealities in the PV model (if the I–V curve representation is model based) or setting up a comprehensive database of measured I–V curves covering as much as possible the nonideal operating conditions to be reproduced (if the I–V curve representation is measurement based).

With reference to this last situation, it is worth observing that several nonideal conditions can be handled during emulation, if different test patterns, corresponding to different evolution of the PV generators under different weather conditions, are available from a database.

As far as the partial shading process is concerned, an example of PV source modeling approach including this phenomenon is described in Sect. 3.5, while Sect. 4.8.3 shows the Matlab<sup>®</sup> implementation of the PV source working under nonuniform illumination.

Khouzam and Hoffman (1996), whose PV emulator is schematized in Fig. 6.8, include in their PV model the effect of radiation damage, due to high energy particles trapped in the Van Allen Belt surrounding the earth. As a matter of fact, these particles penetrate the PV cells, disrupt the ordered lattice and introduce recombination centers, thus reducing the cells' performance.

A simplified modeling of the radiation damage is obtained by introducing the concept of an equivalent fluence, intended as the total number of monoenergetic particles per unit area producing the same level of damage as a spectrum of light particles. Using a the quantity of 1 MeV electrons, the effect of a particle on the short-circuit current of the PV cell is described by Eq. (6.11), due to Lush and Gray (1986).

$$I_{sc|\psi} = I_{sc0} - C_i \log \left[ 1 + \frac{\psi}{\psi_x} \right] \quad (6.11)$$

where  $\psi$  is the irradiation fluence,  $\psi_x$  is the estimated fluence at the end of life (EOL) of the PV cell,  $I_{sc0}$  is the short-circuit current density in (mA/m<sup>2</sup>) at the beginning of life (BOL) of the cell, i.e. at  $\psi = 0$ ,  $I_{sc|\psi}$  is the short-circuit current density in (mA/m<sup>2</sup>) at a fluence of  $\psi$  and  $C_i$  is a constant depending on the type of PV source.

A similar relationship for describing the voltage degradation has been proposed by Khouzam (1988) and used in voltage modeling by Lillington (1988), according to Eq. (6.12).

$$V_{oc} = V_{oc0} - C_v \log \left[ 1 + \left( \frac{\psi}{\psi_x} \right)^{0.8} \right] \quad (6.12)$$

where  $V_{oc0}$  is the open circuit voltage at BOL,  $V_{oc}$  is the open circuit voltage at a fluence  $\psi$  and  $C_v$  is a constant depending on the type of PV source.

Implementing Eqs. (6.11) and (6.12) in the equations that describe the PV model, an I–V curve representation for a PV generator including the radiation damage effect is obtained.

## 6.5 Rated Power

The output power capability of a PV emulator is related to the rated power of the power amplifier. In particular, the power capability can be increased by increasing its size.

On the other hand, in case of DC/DC switching converters, if power switching devices with power limitation at high switching frequencies are used, the output power of a PV emulator can be increased by using several, high switching frequency DC/DC converter units, in suitable connections, according to a modular concept.

In both cases, the use of a control unit only depending on the I–V relationship of the PV source to be emulated is particularly appreciable. As a matter of fact, if the control unit is not dependent on the power converter rated power, it is not required to be modified if the PV emulator capability is changed.

The technical literature exhibits switching DC/DC converter-based PV emulators whose rated power ranges between hundreds of W and tens of kW.

High power PV emulators based on controlled linear power sources have been realized as well, but this design implies the setup of bulky equipments in addition to all the necessary tricks to avoid high power dissipation.

## 6.6 Modularity

The desired output of a PV source emulator should be the same as a real PV generator provides to the subsequent conversion chain. On the other hand, the real PV source could be formed of a series/parallel connection of PV elementary cells or modules.

In order to obtain the maximum flexibility of the PV emulator in terms of current and voltage covered range, some authors introduce in the emulator's design the concept of modularity.

Modularity is a feature related to the possibility of increasing the voltage and current capabilities in an analogous way in which the number of PV emulation units is increased.

In other words, modularity means that additional PV modules or fields can be simulated by adding emulation units in series, if an increased voltage is required,



or in parallel, if an increased current is needed. This feature allows, for example, a series of PV modules to be emulated by the series connection of the same number of emulators where each one implements the model of the module that can be subject to different solar irradiance, reproducing partial shading situations, as well.

The modular approach is promising and has been successfully adopted both within PV high power emulator based on linear amplifiers and on switching power converters.

## 6.7 Examples of Solutions Available on the Market

In addition to the PV emulators described in the technical literature, manufacturers have proposed different solutions for the PV source emulation, generally called Solar Array Simulators (SAS).

They usually adopt the concept of modularity, described in the previous section and consist of programmable DC power supplies which can be operated as individual equipment or in multi-channel configurations to meet higher power ratings requirements, according to a customized turn-key approach.

As an example, two PV emulator systems, proposed respectively by Elgar (Ametek) and Agilent, are described hereinafter.

The Elgar TerraSAS (TSAS) is a PV source emulator providing a turn-key approach to testing the MPPT characteristics for grid-connected inverters and DC charge controllers.

The TSAS encompasses: programmable DC power supplies, a rack mounted controller, a keyboard, and a LCD display with control software and a local graphical user interface (GUI), output isolation and a PV simulation engine controlling the power supply. Thanks to this hardware structure, the TSAS can simulate most of test protocols or combination of events that a solar installation will be subjected to.

The key features of this system can be summarized as follows:

- Dynamic emulation of irradiance and temperature ranging from a clear day to cloud cover conditions;
- Possibility to ramp the voltage, temperature or irradiance level over a programmed time interval;
- Read-back of voltage, current, irradiance level, and temperature setting;
- Tests for inverter Maximum Power Point Tracking (MPPT);
- Programmable I–V curves available for PV Inverter testing;
- Emulation of different types of solar cell material;
- Multi-Channel, up to 1 MW, with power supplies available in 1–15 kW increments.

The required performance for this PV emulator is obtained by high speed switching power supplies using Power MOSFETs, which typically switch very fastly. Higher switching frequency allows smaller output capacitors and inductors to be used, which is the key to an optimal high speed power supply design.

In Fig. 6.19 a photo of the TSAS is given.

**Fig. 6.19** View of the Elgar TerraSAS system (From Elgar TerraSAS. (Online) Available [http://www.elgar.com/go/ts/TerraSAS\\_Datasheet\\_031910.pdf](http://www.elgar.com/go/ts/TerraSAS_Datasheet_031910.pdf))



An advantage of this system is its modularity consisting in building blocks which can be programmed by means of four parameters accounting for the I–V curve endpoints and for the current and voltage mode curve slopes.

More precisely, the only parameters required for a simulation are the open circuit voltage and short-circuit current, while the slope of the I–V curve can then be modified by the peak power parameters,  $V_{MPP}$  and  $I_{MPP}$ .

Changes to these parameters allow the shape of the I–V curve to be adapted to any fill factor between 0.5 and 1.

Once an I–V curve has been generated, changes to the irradiance or temperature level can be imposed by the operator so to test the behavior of a grid-connected inverter under realistic conditions. In general, PV inverters can be optimized for real MPP search modes, because shadowing and temperature changes can be simulated realistically.

The PV simulator has the ability to simulate both ideal I–V curves and irregular characteristics for peak power tracking when solar panels with different output characteristics are parallel connected.

With the PV emulator programmed for different values of irradiance or temperature, the characteristic “multiple hump” I–V curve will result.

By programming the changes in irradiance and temperature in a table, dynamic simulation of compressed time profiles of a 24 h day can be run in a loop to simulate the alternation of day and night for long periods of time.

Long-term weather simulations can be run as well to determine the amount of energy delivered in a given situation.

The Agilent E4360 Modular SAS is a dual output programmable DC power source that performs the emulation of solar arrays under different conditions.

The E4360 SAS is basically a current source with very low output capacitance. It provides up to two outputs and up to 1.2 kW in a small mainframe.

This system is either available as an off-the-shelf instrument to be used as individual equipment or integrated into a full turn-key SAS system configured to meet the exact required specifications. For example, if greater output power and current are needed, the emulator units can be easily operated in parallel thanks to a firmware-based feature that allows the two unit channels to be treated as a single, synchronized channel with twice the output current, and power capability.

The key features of this SAS system are the following:

- Accurate emulation of any type of solar array;
- Small size;
- Modularity;
- Output power up to 600 W per output;
- Fast I–V curve change and fast recovery switching time;
- Easy to simulate environmental conditions;
- LAN, USB, and GPIB interfaces.

In Fig. 6.20 an example of a custom turn-key E4360 SAS-based system is illustrated.

The E4360 SAS provides three operating modes, i.e., simulator (SAS) mode, table mode, and fixed mode.

In particular, if the I–V curve of a PV generator has to be emulated, SAS or table modes are used. On the contrary, if a standard power supply is needed, fixed mode is used.

In simulator (SAS) mode, the E4360 SAS generates a I–V point table on the basis of an internal algorithm which approximates the I–V curve. This can be done via the I/O interfaces or from the front panel, where a PC is not needed. In order to establish a I–V curve in this mode, open circuit voltage, short-circuit current, and MPP are needed.

In table mode, the I–V curve is determined by a user-defined table of points with a minimum of three points, up to a maximum of 4000 points.

Up to 30 tables can be stored in each of the E4360 SAS built-in volatile and nonvolatile memory.

Current and voltage offsets can be applied to the selected Table (I–V curve) to simulate a change in the operating conditions of the PV generator.

Finally, fixed mode is the default mode when the unit is powered on. In this case, the unit has the rectangular I–V characteristics of a standard power supply.

Notwithstanding the certain value of such commercial solutions, their cost, especially for the emulation of high power PV generators, could represent a key point.

**Fig. 6.20** Custom turn-key E4360 SAS-based system (From Agilent E4360 Modular solar array simulators, datasheet. (Online) Available <http://cp.literature.agilent.com/litweb/pdf/5989-8485EN.pdf>)



## 6.8 Conclusions

Photovoltaic industry is growing exponentially and the availability of specialized equipment for the laboratory emulation of PV generators is becoming essential for manufacturers and laboratories working in the field of PV plant-associated power electronics. In particular, since the trend moves toward more efficient PV inverters, the setup of effective and reliable PV emulators is becoming more and more a challenging issue.

The need of reproducing in laboratory the PV source behavior has been recognized since the end of 1970s. Several solutions have been devised. Firstly, emulators were based on a physical sample of the PV source and on operational amplifiers; then, more sophisticated models implemented on computers and power circuits based either on linear regulators or switching DC/DC converter have been proposed.

The emulators based on linear regulators are not affected by noise due to PWM operation and have a good dynamic behavior but their low efficiency requires good heatsink systems or variable DC supplies that could worsen the dynamics.

On the contrary, emulators based on switching DC/DC converters can deliver high powers with a good dynamic behavior by a correct choice of the switching frequency and of the feedback network.

This chapter presents a survey of PV emulators which have been proposed in the technical literature, including some examples of commercial solutions.

The most critical aspects related to PV emulators design and operation are put in evidence, such as power stage schemes, control features, dynamics, modularity, and so on. It has been definitely observed that the more common and promising modern PV emulators are realized by DC/DC switching converters, with output regulation based on suitable I–V curve representation.

On the basis of such elements, an indepth examination of the main topologies of DC/DC converters and of their related control techniques is considered particularly useful and will be the object of the next chapters.

## Bibliography

- Agilent E4360 Modular Solar Array Simulators, Models: E4360-62A, E4366-68A, Datasheet. (Online) Available <http://cp.literature.agilent.com/litweb/pdf/5989-8485EN.pdf>
- Baert D (1979) Solar-cell panel simulation. *Electron lett* 15(2)
- Bazzi AM, Klein Z, Sweeney M, Kroeger KP, Shenoy PS, Krein PT (2012) Solid-state solar simulator. *IEEE Trans Ind Appl* 48(4):1195–1202
- Di Piazza MC, Vitale G (2010) Photovoltaic field emulation including dynamic and partial shadow conditions. *Appl Energy* 3(87):814–823
- Elgar TerraSAS—Programmable Solar Array Simulator. (Online) Available [http://www.elgar.com/go/ts/TerraSAS\\_Datasheet\\_031910.pdf](http://www.elgar.com/go/ts/TerraSAS_Datasheet_031910.pdf)
- Haeblerlin H, Borgna L (2004) A new approach for semi-automate measurement of PV inverters, especially MPP tracking efficiency, using linear PV array simulator with high stability. In: *Proceedings 19th European photovoltaic solar energy conference*, 2332–2336
- Koutroulis E, Kalaitzakis K, Tzitzilonis V (2009) Development of an FPGA-based system for real-time simulation of photovoltaic modules. *Microelectron J* (40):1094–1102
- Kouzam K, Hoffman K (1996) Real-time simulation of photovoltaic modules. *Sol Energy* 6(56):521–526
- Lloyd SH, Smith GA, Infield DG (2000) Design and construction of a modular electronic photovoltaic simulator. In: *Proceedings 8th international conference on power electronics and variable speed drives*, 120–123
- Luque A, Hegedus S (eds) (2003) *Handbook of photovoltaic science and engineering*. Wiley, Hoboken
- Martín-Segura G, Lopez-Mestre J, Teixido-Casas M, Sudria-Andreu A, (2007) Development of a photovoltaic array simulator system based on a full-bridge structure. In: *Proceedings 9th international conference electrical power quality and utilisation*, 1–6
- Matsukawa H, Koshiishi K, Koizumi H, Kurokawa K, Hamada M, Bo L (2003) Solar Energy mat solar cells (75):537–546
- Mukerjee AK, Dasgupta N (2007) DC power supply used as photovoltaic simulator for testing MPPT algorithms. *Renewable Energy* (32):587–592

- Nagayoshi H (2004) I-V curve simulation by multi-module simulator using I-V magnifier circuit. *Sol Energy Mater Sol Cells* (82):159–167
- Ollila J (1995) A medium power PV-array simulator with a robust control strategy. In: *Proceedings IEEE power electronic special conference* 40–45
- Sanchis P, Echeverria I, Ursua A, Alonso E, Gubia E, Marroyo L (2003) On the testing characterization, and evaluation of PV inverters and dynamic MPPT performance under real varying operating conditions. *Prog Photovolt Res Appl* (15):541–556
- Solanki SC, Dubey S, Tiwari A (2009) Indoor simulation and testing of photovoltaic thermal (PV/T) air collectors. *Appl Energy* (86):2421–2428
- Tiwari A, Barnwal P, Sandhu G, Sodha MS (2009) Energy metrics analysis of hybrid photovoltaic (PV) modules. *Appl Energy* (86):2615–2625
- Zeng Q, Song P, Chang L (2002) A photovoltaic simulator based on a DC chopper. In: *Proceedings of the 2002 IEEE canadian conference on electrical and computer engineering*, 257–261